

PDF hosted at the Radboud Repository of the Radboud University Nijmegen

The following full text is a publisher's version.

For additional information about this publication click this link.

<http://repository.ubn.ru.nl/handle/2066/127870>

Please be advised that this information was generated on 2018-07-07 and may be subject to change.

Irreversible modification of magnetic properties of Pt/Co/Pt ultrathin films by femtosecond laser pulses

J. Kisielewski, W. Dobrogowski, Z. Kurant, A. Stupakiewicz, M. Tekielak, A. Kirilyuk, A. Kimel, Th. Rasing, L. T. Baczewski, A. Wawro, K. Balin, J. Szade, and A. Maziewski

Citation: *Journal of Applied Physics* **115**, 053906 (2014); doi: 10.1063/1.4864068

View online: <http://dx.doi.org/10.1063/1.4864068>

View Table of Contents: <http://scitation.aip.org/content/aip/journal/jap/115/5?ver=pdfcov>

Published by the [AIP Publishing](#)

Articles you may be interested in

[Spin reorientation transition and phase diagram in an He⁺ ion irradiated ultrathin Pt/Co\(0.5 nm\)/Pt film](#)
J. Appl. Phys. **108**, 103915 (2010); 10.1063/1.3514086

[Structure and magnetism of ultrathin Co film grown on Pt\(100\)](#)
J. Vac. Sci. Technol. A **23**, 790 (2005); 10.1116/1.1885025

[Magnetic properties of ultrathin Ni/Co/Pt\(111\) films](#)
J. Appl. Phys. **95**, 6568 (2004); 10.1063/1.1683011

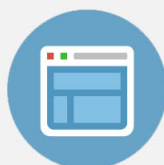
[Magnetic properties of ultrathin Co/Ag/Pt\(111\) films](#)
J. Appl. Phys. **94**, 5873 (2003); 10.1063/1.1614868

[Giant enhancement of magneto-optical response and increase in perpendicular magnetic anisotropy of ultrathin Co/Pt\(111\) films upon thermal annealing](#)
J. Vac. Sci. Technol. A **17**, 3045 (1999); 10.1116/1.582003



Re-register for Table of Content Alerts

Create a profile.



Sign up today!



Irreversible modification of magnetic properties of Pt/Co/Pt ultrathin films by femtosecond laser pulses

J. Kisielewski,^{1,2,a)} W. Dobrogowski,² Z. Kurant,² A. Stupakiewicz,² M. Tekielak,² A. Kirilyuk,¹ A. Kimel,¹ Th. Rasing,¹ L. T. Baczewski,³ A. Wawro,³ K. Balin,⁴ J. Szade,⁴ and A. Maziewski²

¹*Institute for Molecules and Materials, Radboud University Nijmegen, Heyendaalseweg 135, 6525AJ Nijmegen, The Netherlands*

²*Laboratory of Magnetism, University of Białystok, Lipowa 41, 15-424 Białystok, Poland*

³*Institute of Physics, Polish Academy of Sciences, al. Lotników 32/46, 02-668 Warsaw, Poland*

⁴*A. Chełkowski Institute of Physics, University of Silesia, Uniwersytecka 4, 40-007 Katowice, Poland*

(Received 18 December 2013; accepted 22 January 2014; published online 4 February 2014)

Annealing ultrathin Pt/Co/Pt films with single femtosecond laser pulses leads to irreversible spin-reorientation transitions and an amplification of the magneto-optical Kerr rotation. The effect was studied as a function of the Co thickness and the pulse fluence, revealing two-dimensional diagrams of magnetic properties. While increasing the fluence, the creation of two branches of the out-of-plane magnetization state was found. © 2014 AIP Publishing LLC.

[<http://dx.doi.org/10.1063/1.4864068>]

I. INTRODUCTION

The magnetic anisotropy, a quantity that controls the preferred direction of the magnetization in magnetic media, is crucial in studies of magnetism, in general, and in particular for practical applications in magnetic devices. It determines both static properties, such as the stability of magnetic bits persisting for years,¹ and the switching dynamics of such bits on a sub-nanosecond time scale.² Apart from the magnetocrystalline anisotropy, the surface and shape contributions to the anisotropy play also an important role in nanostructures. This interplay leads under certain conditions to a spin-reorientation transition (SRT)—a change of preferred magnetization direction, that may occur as a function of layer thickness³ or temperature.⁴

One of the ways of changing the magnetic anisotropy of ultrathin films is affecting the surface contribution to the anisotropy, connected with the quality of the interfaces. Treating the sample thermally may lead, depending on the used materials, to improvement or degradation of that quality. For Pt/Co/Pt interfaces, due to a large negative enthalpy of alloy formation at elevated temperature,⁵ annealing leads to intermixing of atoms in neighboring layers,⁶ followed by a decrease of the magnetic anisotropy.^{7,8} On the contrary, initially poor interfaces of Au/Co/Au structures can be improved by annealing (due to immiscibility of Co and Au), resulting in a creation of the out-of-plane magnetic phase.⁹ Ion-irradiation is another example of a technique which can change magnetic properties, affecting strongly the interfaces. The observed irradiation-driven decrease of the magnetic anisotropy and coercivity in Co-Pt sandwiches and multilayers^{10,11} was interpreted in terms of a degradation of the quality of the interface. Recently, addition to this effect, the appearance of two out-of-plane magnetic phases was

observed with increasing irradiating ion fluence, for Ga-irradiated Pt/Co/Pt layers.^{12,13}

As light also carries energy, it may increase the temperature in metals due to absorption. For low energies of light pulses, the thermally induced changes of the magnetization and magnetic anisotropy are reversible and may trigger a magnetization precession,^{14,15} while with higher light intensities, irreversible changes of the structure can be achieved. Employing few-nanosecond laser pulses, a decrease of the magnetic anisotropy in Pt/Co/Pt systems^{16,17} was observed; on the contrary, for Au/Co/Au the possibility of creating the out-of-plane magnetization state with semi-continuous laser irradiation was demonstrated.¹⁸ The reported effects of such laser-annealing were consistent with thermal annealing as discussed above.⁷⁻⁹

In this paper, the results of single ultrashort laser pulse-induced modifications of the magnetic anisotropy and magneto-optical effects in ultrathin Pt/Co/Pt films are presented. We demonstrate the effect of the creation of a permanent out-of-plane magnetization phase above the SRT thickness, where originally the in-plane state occurs. In contrast to the experiments mentioned above (Refs. 16–18), we used laser pulses of 60 fs duration, which allowed us to get very clear patterns, not blurred by planar heat diffusion, with a structure directly related to the spatial distribution of the energy density of the laser pulses. The studies, carried out systematically with various pulse energies and Co layer thicknesses, revealed a complex phase diagram, containing out-of-plane and in-plane regions and numerous reorientation transitions in between.

II. EXPERIMENTAL DETAILS

The sample, composed of Pt(5 nm)/Co(wedge: 1.5–5 nm)/Pt(5 nm), was deposited onto a sapphire (0001) substrate, using molecular beam epitaxy, in a pressure of 10^{-10} Torr. Epitaxial growth was monitored *in situ* by RHEED technique.

^{a)}Electronic mail: jankis@uwb.edu.pl

The Co layer was found to grow in *hcp* structure with (0001) orientation, the Pt layers in *fcc* structure with (111) orientation. The as-deposited structure was initially characterized with a magneto-optical Kerr effect (MOKE) millimagnetometer and the thickness of the SRT, $d_{\text{SRT}} = 2.4$ nm, was determined. The laser annealing procedure was carried out with single pulses of a Ti:sapphire oscillator, amplified with a regenerative amplifier with a repetition rate of 1 kHz. Laser pulses of wavelength of 800 nm, duration of 60 fs, and energy in the range of 1.3–4.6 μJ (measured carefully with a power meter working in a single pulse mode) were focused at the sample surface with a lens. Determining the beam radius with the knife-edge method^{19,20} showed that the spatial profile of the beam used in our experiment is fitted well with a sum of two Gaussian profiles.²¹ The radii of both Gaussian components were equal to: $r_1 = (33.8 \pm 0.5)\mu\text{m}$, $r_2 = (217 \pm 21)\mu\text{m}$, with a dominant contribution of $(98.6 \pm 0.4)\%$ of the first one. Amplitudes of the energy density distributions, in the range of 22–82 mJ/cm^2 for different pulse energies, were obtained using the fact, that the integral of the energy density over the two-dimensional space yields the total pulse energy, measured in the experiment. A chopper, synchronized with the output laser frequency, allowed to release manually single laser pulses. In this way, changing the initial pulse energy with neutral density filters, and moving the sample after each released pulse, an array of annealed spots was created at the sample surface, as a function of pulse energy and Co thickness (with a step of 0.1 nm).

Characterization of the magnetic properties of the irradiated regions was done with a specially constructed Kerr microscope in the polar configurations (PMOKE). Images were registered in two following experimental options: (i) *the remanence images* were obtained as a difference between two images taken after field pulses of opposite amplitudes ± 4 kOe, applied perpendicularly to the sample surface (any non-zero remanence results in non-zero difference between the images, visible as bright color); (ii) at the field sweeping between ± 4 kOe, this option enabled determination of a magnetization curve. The pixel intensity in the registered image was proportional to the local Kerr rotation, Θ , which is further related to the out-of-plane component of the magnetization, as well as the magneto-optical constants. The spatial resolution available in options (i) and (ii) was 0.7 and 0.2 $\mu\text{m}/\text{pixel}$, respectively—in both cases, beyond the theoretical diffraction limit of the system. Additionally, some regions of the sample were studied with a Kerr microscope in the longitudinal configuration (LMOKE), with the sweeping magnetic field applied parallel to the sample plane.

III. RESULTS

The PMOKE remanence images of the sample and selected spots are shown in Figure 1. The local pixel intensity, coded with the color scale, was calculated dividing the polar Kerr rotation at zero field, Θ_R , by the maximal Kerr rotation in the studied region of the as-deposited structure, Θ_{S0} . This way the background of each image corresponds to the initial perpendicular ($\Theta_R/\Theta_{S0} = 1$, light blue) or parallel ($\Theta_R/\Theta_{S0} = 0$, black) magnetization state, below and above

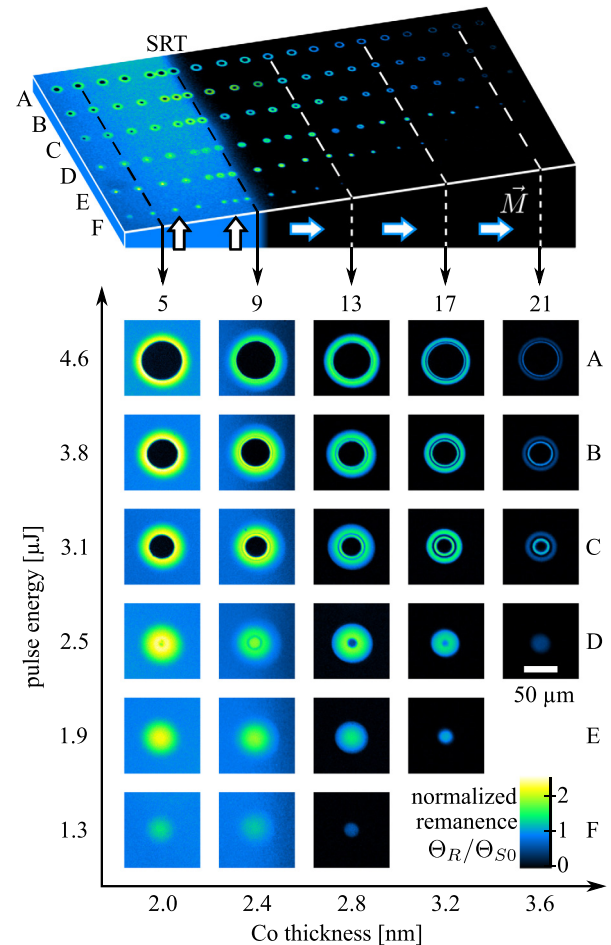


FIG. 1. Normalized remanence images (Θ_R/Θ_{S0}) of the sample (top) and selected laser-annealed spots, as a function of Co thickness and pulse energy. The spots are labeled with a combination of a capital letter (A–F, at the right) for the “rows” of constant pulse energy and a number (5–21, at the top), for the “columns” of constant Co thickness.

the SRT thickness, respectively. The most striking result is the occurrence of bright ring- or disk-shaped objects above the SRT thickness, which means the creation of the out-of-plane magnetization phase. Moreover, appearing objects exhibit $\Theta_R/\Theta_{S0} > 1$ (the colors brighter than light blue), indicating an enhanced magneto-optical signal (Θ_S).

Figure 2 displays the hysteresis curves measured for the most characteristic regions of the spots A5 ($d < d_{\text{SRT}}$) and C17 ($d > d_{\text{SRT}}$). Considering the shape of the hysteresis loops, one can determine a variation of the preferred magnetization phase across the spot. Particularly, the PMOKE remanence Θ_R divided by the local saturation Θ_S is equal to the average cosine of the magnetization orientation angle, counted from the sample normal. Going from the as-deposited region to the central part of the spot A5, one can find the evolution of the magnetic and magneto-optical properties: an increase of coercivity and Θ_S , and then a transition from the perpendicular to the in-plane magnetization state, manifested by a hard-axis-type of PMOKE hysteresis loop and a square LMOKE loop. Quite new light-induced effects appear for the spot C17. The creation of two concentric rings of the out-of-plane magnetization phase is visible. The rings are separated

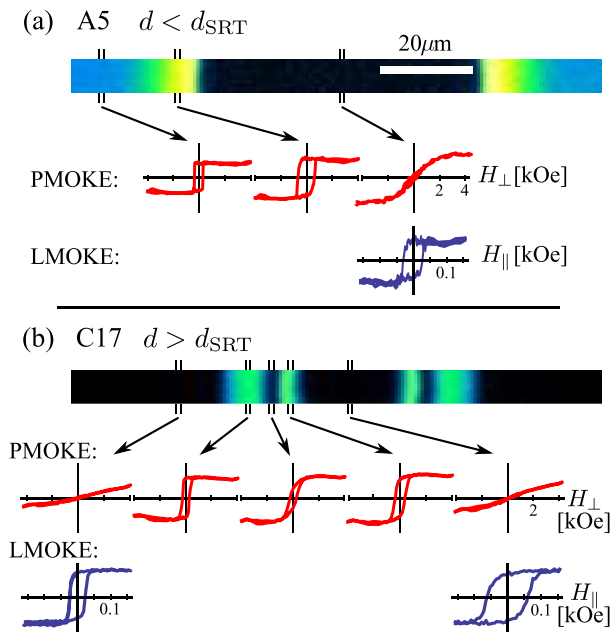


FIG. 2. Examples of the hysteresis curves for the most characteristic regions of two selected spots: (a) A5 ($d < d_{\text{SRT}}$) and (b) C17 ($d > d_{\text{SRT}}$). The PMOKE curves were averaged over rectangles of 1×15 pixels from respective areas of the spot, the LMOKE curves—over bigger areas of about $15 \mu\text{m}$ in diameter. Vertical scales are conserved, separately for (a) and (b), and for PMOKE and LMOKE curves.

by a region, where the out-of-plane component is weaker, but still present, what may indicate an easy-cone magnetization state. In the central part of the spot, the magnetization prefers the in-plane orientation.

IV. DISCUSSION

The variety of annealed spots structures, depending on the Co thickness and the light pulse energy, demonstrates the high complexity of the problem. Attempting to systematize it, we start with a simple observation. All images have a perfect rotational symmetry, connected with the symmetry of the irradiating laser pulses. Within the laser pulse, the spatial distribution of the energy density is described with the above mentioned two-dimensional Gaussian shapes. This suggests a connection between the local energy density and the local changes of the magnetic properties. Such connection can be made only if no planar energy transfer is assumed. This is reasonable, as due to the large planar size of the beam (micrometers) in comparison with the thickness of the sample (nanometers), the planar energy distribution on the nanometer-scale is almost homogeneous and the substrate is expected to be a main channel of energy dissipation in the direction perpendicular to the sample surface. Details of the modeling of the temperature dynamics are discussed in Ref. 15. Crucial here is also the absence of the long-term heat transfer resulting from heat accumulation. This is ensured by the ultrashort pulse duration—shorter than the process of heating the system up, which in ultrathin metallic structures usually takes a few picoseconds.²²

The mentioned connection between the energy density and the remanence is presented in Figures 3(a) and 3(b), for

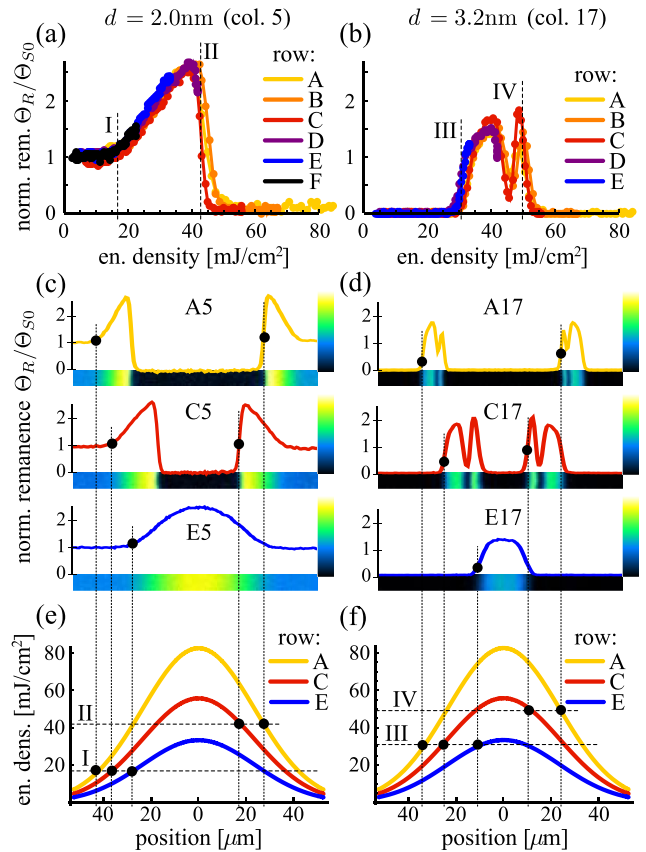


FIG. 3. (a) and (b) The normalized remanence (Θ_R/Θ_{S0}) as a function of the laser energy density, determined for the Co thickness of (a) 2.0 nm (below d_{SRT} , column 5) and (b) 3.2 nm (above d_{SRT} , column 17). The analysis was performed using the data from spots A5–F5 and A17–E17, respectively. The idea of the construction is explained in (c)–(f): exemplary profiles of the normalized remanence for the spots (c) A5, C5, E5 and (d) A17, C17, E17 were combined with (e) and (f) respective profiles of the energy density, for rows A, C, and E. Some characteristic energy densities are marked with the lines I–IV.

the Co thicknesses of 2.0 and 3.2 nm (columns 5 and 17), respectively. The method of the construction of those plots is explained in Figures 3(c)–3(f). First, a profile of the remanence image across the spot's center (Figures 3(c) and 3(d)) is taken. Next, for each pixel of this profile we calculate the local energy density, using the respective Gaussian distributions (Figures 3(e) and 3(f)). Considering the different total pulse energies (rows A–F), a certain local energy density occurs at a different distance from the spot's center. This results in different sizes of laser-induced structures—to illustrate this fact, some characteristic energy densities, corresponding to the inner and outer edges of the spots, are marked with the lines I–IV. Finally, pairs of numbers (the local energy density and the remanence), collected from each pixel of the profile, yield a desired dependence (Figures 3(a) and 3(b)). For a given Co thickness, curves for various pulse energies reproduce exactly the same dependence, however, covering different ranges, as the accessible energy density range is different in the pulses of different total energies.

This “common” dependence changes with Co thickness, and these two parameters (local energy density and the thickness) prove to be enough to describe the modification of the magnetic state by the laser pulses. Such two-dimensional

dependence of the remanence is depicted in the form of a two-dimensional diagram in Figure 4. That diagram shows in a concise way the magnetization state that can be induced in a Co layer of a given thickness, by applying a laser pulse with a given local energy density. Below the SRT thickness, the magneto-optical signal is significantly increased (the color becomes brighter with increasing energy density). Above the SRT thickness and above a certain threshold energy density (depending on the thickness), two out-of-plane magnetization phases emerge, manifested in two “branches,” separated with a region of a lower average cosine of magnetization orientation angle. The upper branch of the out-of-plane magnetization phase spreads over the Co thicknesses up to about 4.3 nm. Above a certain thickness-dependent boundary energy density, for the whole range of thicknesses, the in-plane magnetization phase appears.

The here reported laser-induced transition from the out-of-plane to the in-plane magnetic phase, occurring for the highest pulse energy densities, is similar to that previously described in Refs. 16 and 17. On the other hand, the open question is: what structural changes, driven by laser pulses of moderate energy densities, are responsible for the observed creation of the two out-of-plane magnetic phases with the enhanced magneto-optical signal? An analogous effect, but with one out-of-plane phase only, was observed *in situ* using a standard furnace annealing of Co/Pt system.²³ The given explanation concerned the formation of Co-Pt alloys at the interface. In order to answer that question, at first the atomic force microscopy (AFM) studies of some selected laser-annealed spots were performed, manifesting a lack of significant changes in the sample topography in the area where the out-of-plane magnetization phase was

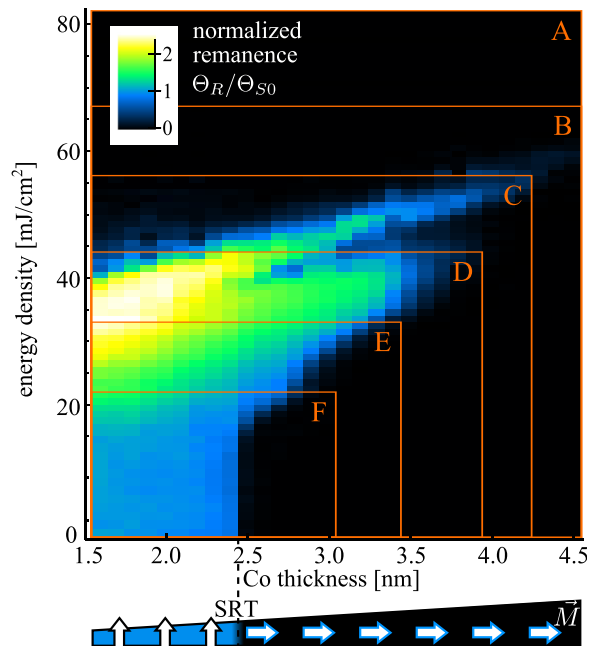


FIG. 4. Two-dimensional diagram of the normalized remanence (Θ_R/Θ_{S0}), derived from the series of remanence images, as a function of Co thickness and local energy density of the annealing laser pulses. Zero energy density corresponds to the as-deposited structure. The orange frames mark the ranges that are accessible with laser pulses of the rows A–F.

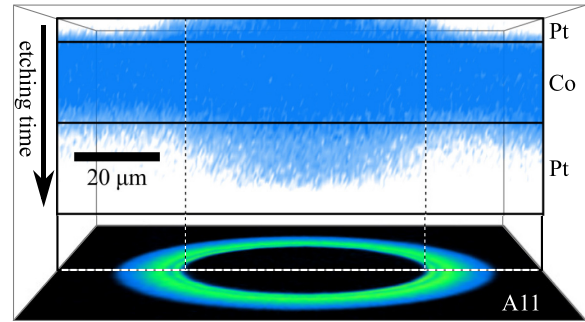


FIG. 5. The distribution of Co obtained from the ToF-SIMS measurements—the cross-section through the center of the irradiated spot A11, related to the remanence image at the bottom. The vertical axis corresponds to the etching time. Due to various etching rates within the layers, the depth-scale is strongly non-linear; however, the relative changes of the Co concentrations in the Pt layers are clearly visible.

induced. To check the local chemical variation caused by the irradiation, we also performed the 3D time of flight secondary ion mass spectroscopy (ToF-SIMS) studies of the region of the spot A11 with the surrounding unaffected area. Figure 5 shows the distribution of the collected secondary Co^+ ions across the spot. There is a clear increase of the Co concentration in the region of the spot, visible within both the upper and lower Pt layers.

The Co-Pt alloys, due to hybridization of electron orbitals and induced large magnetic moments on Pt atoms, exhibit an enhanced spin-orbit interaction, which is the origin of both the enhanced magnetic anisotropy and the enhanced Kerr effect.²⁴ In fact, a correlation between these two quantities is found in our results. The magnetic properties of the Co-Pt alloys strongly depend on concentration,²⁵ crystallographic structure,²⁶ as well as a degree of order.²⁷ As the laser excitation takes extremely short time, non-equilibrium thermodynamical processes may occur, making the structure more complex, through a creation of various Co-Pt alloy phases, exhibiting a strong magnetic anisotropy. The similar effect was obtained by ion-irradiation,^{12,13,28} and also interpreted in terms of formation of ordered alloys or ion-induced stresses.²⁹ In both techniques (light- and ion-irradiation), there is a transfer of energy to the sample, and despite the fact that the channels of this transfer are different, possibly similar mechanisms of structure modification may occur. To decide, which scenario is realized in our case and what alloy phases are responsible for the induced out-of-plane magnetization states, further microscopic investigations are necessary. Unfortunately, the fact that the light-induced changes take place at buried interfaces, and moreover within a planarly confined area, eliminates the techniques typically used for an *in situ* characterization of the surface structure, such as STM, RHEED, LEED, AES, or XPS.

V. CONCLUSIONS

To conclude, femtosecond laser-induced irreversible modifications of the magnetic anisotropy in ultrathin Pt/Co/Pt systems are reported. Out-of-plane magnetization phases, with increased coercivity and larger magneto-optical

response, were found to be created permanently for the Co layer thicknesses far above the SRT thickness, for a certain range of energy density of irradiating laser pulses. Connecting the local energy density distribution with the structure of the annealed objects allowed to create two-dimensional diagrams of the light-induced changes of the magnetic properties. The demonstrated effects open the opportunity to produce perpendicularly magnetized nanostructures in a desired way, using relatively simple methods, like interference lithography.³⁰ On the other hand, new interesting experimental and theoretical tasks are appearing, in the context of the light-induced structural changes or mechanisms of anisotropy alteration.

ACKNOWLEDGMENTS

The authors thank Iosif Sveklo for sample characterization by AFM technique. The work was partially sponsored by: ITN FANTOMAS (Grant No. 214810) and the European Research Council (Grant No. 257280, Femtomagnetism), both under EU FP7/2007–2013; SYMPHONY project (Polish Science Team Programme, European Regional Development Fund, OPIE 2007–2013); the National Science Centre Poland (DEC-2012106/M/ST3/00475); De Nederlandse Organisatie voor Wetenschappelijk Onderzoek (NWO).

- ¹D. Sellmyer, M. Yan, Y. Xu, and R. Skomski, *IEEE Trans. Magn.* **41**, 560 (2005).
- ²T. Gerrits, H. A. M. van den Berg, J. Hohlfeld, L. Bar, and T. Rasing, *Nature* **418**, 509 (2002).
- ³W. J. M. de Jonge, P. J. H. Bloemen, and F. J. A. den Broeder, "Experimental investigations of magnetic anisotropy," in *Ultrathin Magnetic Structures* (Springer-Verlag, 1994).
- ⁴D. P. Pappas, K.-P. Kämper, and H. Hopster, *Phys. Rev. Lett.* **64**, 3179 (1990).
- ⁵R. Oriani and W. Murphy, *Acta Metall.* **10**, 879 (1962).
- ⁶M. Galeotti, A. Atrei, U. Bardi, B. Cortigiani, G. Roviada, and M. Torrini, *Surf. Sci.* **297**, 202 (1993).
- ⁷H. J. G. Draaisma, F. J. A. den Broeder, and W. J. M. de Jonge, *J. Appl. Phys.* **63**, 3479 (1988).
- ⁸G. A. Bertero, R. Sinclair, C.-H. Park, and Z. X. Shen, *J. Appl. Phys.* **77**, 3953 (1995).

- ⁹F. J. A. den Broeder, D. Kuiper, A. P. van de Mosselaer, and W. Hoving, *Phys. Rev. Lett.* **60**, 2769 (1988).
- ¹⁰C. Chappert, H. Bernas, J. Ferré, V. Kottler, J.-P. Jamet, Y. Chen, E. Cambriil, T. Devolder, F. Rousseaux, V. Mathet *et al.*, *Science* **280**, 1919 (1998).
- ¹¹T. Devolder and H. Bernas, "Magnetic properties and ion beams: Why and how," in *Materials Science With Ion Beams, Topics in Applied Physics* (Springer-Verlag, Berlin, 2010), Vol. 116.
- ¹²J. Jaworowicz, A. Maziewski, P. Mazalski, M. Kisielewski, I. Sveklo, M. Tekielak, V. Zablotnik, J. Ferré, N. Vernier, A. Mougín *et al.*, *Appl. Phys. Lett.* **95**, 022502 (2009).
- ¹³A. Maziewski, P. Mazalski, Z. Kurant, M. O. Liedke, J. McCord, J. Fassbender, J. Ferré, A. Mougín, A. Wawro, L. T. Baczewski *et al.*, *Phys. Rev. B* **85**, 054427 (2012).
- ¹⁴M. van Kampen, C. Jozsa, J. T. Kohlhepp, P. LeClair, L. Lagae, W. J. M. de Jonge, and B. Koopmans, *Phys. Rev. Lett.* **88**, 227201 (2002).
- ¹⁵J. Kisielewski, A. Kirilyuk, A. Stupakiewicz, A. Maziewski, A. Kimel, T. Rasing, L. T. Baczewski, and A. Wawro, *Phys. Rev. B* **85**, 184429 (2012).
- ¹⁶A. Aktag, S. Michalski, L. Yue, R. D. Kirby, and S.-H. Liou, *J. Appl. Phys.* **99**, 093901 (2006).
- ¹⁷C. Schuppler, A. Habenicht, I. L. Guhr, M. Maret, P. Leiderer, J. Boneberg, and M. Albrecht, *Appl. Phys. Lett.* **88**, 012506 (2006).
- ¹⁸J. Kisielewski, K. Postava, I. Sveklo, A. Nedzved, P. Trzciński, A. Maziewski, B. Szymański, M. Urbaniak, and F. Stobiecki, *Solid State Phenom.* **140**, 69 (2008).
- ¹⁹J. M. Khosrofi and B. A. Garetz, *Appl. Opt.* **22**, 3406 (1983).
- ²⁰M. A. C. de Araújo, R. Silva, E. de Lima, D. P. Pereira, and P. C. de Oliveira, *Appl. Opt.* **48**, 393 (2009).
- ²¹J. Chalupský, J. Krzywinski, L. Juha, V. Hájková, J. Cihelka, T. Burian, L. Vyšín, J. Gaudin, A. Gleeson, M. Jurek *et al.*, *Opt. Express* **18**, 27836 (2010).
- ²²E. Beaurepaire, J.-C. Merle, A. Daunois, and J.-Y. Bigot, *Phys. Rev. Lett.* **76**, 4250 (1996).
- ²³M.-T. Lin, C. C. Kuo, H. Y. Her, Y. E. Wu, J. S. Tsay, and C. S. Shern, *J. Vac. Sci. Technol., A* **17**, 3045 (1999).
- ²⁴D. Weller, H. Brändle, and C. Chappert, *J. Magn. Magn. Mater.* **121**, 461 (1993).
- ²⁵P. Pouloupoulos, M. Angelakeris, E. T. Papaioannou, N. K. Flevaris, D. Niarchos, M. Nyvlt, V. Prosser, S. Visnovsky, C. Mueller, P. Fumagalli *et al.*, *J. Appl. Phys.* **94**, 7662 (2003).
- ²⁶H. Sato, T. Shimatsu, Y. Okazaki, H. Muraoka, H. Aoi, S. Okamoto, and O. Kitakami, *J. Appl. Phys.* **103**, 07E114 (2008).
- ²⁷J. M. Sanchez, J. L. Moran-Lopez, C. Leroux, and M. C. Cadeville, *J. Phys. C* **21**, L1091 (1988).
- ²⁸P. Mazalski, Z. Kurant, A. Maziewski, M. O. Liedke, J. Fassbender, L. T. Baczewski, and A. Wawro, *J. Appl. Phys.* **113**, 17C109 (2013).
- ²⁹M. Sakamaki, K. Amemiya, M. O. Liedke, J. Fassbender, P. Mazalski, I. Sveklo, and A. Maziewski, *Phys. Rev. B* **86**, 024418 (2012).
- ³⁰N. I. Polushkin, V. Oliveira, O. Conde, R. Vilar, Y. N. Drozdov, A. Apolinario, A. Garcia-Garcia, J. M. Teixeira, and G. N. Kakazei, *Appl. Phys. Lett.* **101**, 132408 (2012).